# Modeling of Rainfall-Induced Shallow Landslides of the Flow-Type

Leonardo Cascini[1]; Sabatino Cuomo[2]; Manuel Pastor[3]; and Giuseppe Sorbino[4]

**Abstract:** The paper deals with the modeling of failure and postfailure stage of shallow landslides of the flow-type that often affect natural shallow deposits of colluvial, weathered, and pyroclastic origin. The failure stage is frequently associated to rainfall that directly infiltrates the slope surface and to spring from the underlying bedrock. The postfailure stage is characterized by the sudden acceleration of the failed mass. The geomechanical modeling of both stages, based on site conditions and soil mechanical behavior, represents a fundamental issue to properly assess the failure conditions and recognize the potential for long travel distances of the failed soil masses. To this aim, in this paper, the current literature on the failure and postfailure stages of the shallow landslides of the flow-type is first reviewed. Then, an approach for their geomechanical modeling is proposed and three different modeling alternatives are presented. These models are then used to analyze, at different scales, a relevant case study of Southern Italy (Sarno-Quindici event, May 4–5, 1998). Numerical analyses outline that both site conditions and hydraulic boundary conditions are among the key factors to evaluate the reliability of landslides of the flow-type. The potentialities and limitations of the available models are also evidenced as well as the perspectives related to the use of more advanced numerical models.

**DOI:** 10.1061/(ASCE)GT.1943-5606.0000182

**CE Database subject headings:** Landslides; Rainfall; Infiltration; Bedrock; Numerical models.

**Author keywords:** Shallow landslides; Flow-type; Rainfall infiltration; Spring; Bedrock; Modeling.

## Introduction

Landslides of the flow-type (Hungr et al. 2001) often pose significant threats to populations and structures being characterized by long travel distances (hundreds of meters) and high velocities (in the order of meters/second) (Schuster and Highland 2007). They can be triggered in many geoenvironmental contexts by a number of natural and/or anthropogenic factors. In natural hillslopes one of the most frequent triggering factors is represented by rainfall (De Vita and Reichenbach 1998) that can directly infiltrate the slope surface or can indirectly provide subsurface water supplies from the bedrock. Due to the usual large extension of the rainfall events, these landslides can be triggered over large areas (up to tens of square kilometers) and they generally involve shallow soil deposit of different grading and origin. Significant examples are frequently recorded in pyroclastic deposits in Central America (Capra et al. 2003) and New Zealand (Ekanayake and Philipps 2002), in situ weathered soils in Hong Kong (Take et al. 2004) and Japan (Wang et al. 2002), colluvial weathered deposits in Brazil (Lacerda 2004) and Hong Kong (Fuchu et al. 1999).

These landslides can be considered complex slope instability phenomena since they exhibit distinct kinematic characteristics during the failure, postfailure and propagation stages (Fell et al. 2000; Hungr et al. 2001; Pastor et al. 2002; Leroueil 2004). Failure and postfailure stages occur inside the so-called landslide source areas. Failure stage is characterized by the formation of a continuous shear surface through the entire soil mass (Leroueil 2001). Postfailure stage is represented by the rapid generation of large plastic strains and the consequent sudden acceleration of the failed soil mass (Hungr 2004). Propagation stage includes movement of the failed soil mass from the landslide source areas to the deposition areas, where the failed soil mass stops. With reference to the failure stage, these rainfall-induced shallow landslides of the flow-type can be classified as translational slides in the classifications of landslides proposed by Hutchinson (1988) and Cruden and Varnes (1996). As for the postfailure stage, they can be classified simply as landslides of the flow-type (Hungr et al. 2001) (i.e., slides turning into flows) or as flowslides (Hungr et al. 2001) when liquefaction phenomena occur.

Considering the destructiveness of these landslides, the geomechanical modeling of the mechanisms occurring inside the source areas can be particularly useful in the hazard estimation as it contributes to the assessment of the landsliding volumes and their potential for traveling long distances. However, this issue certainly poses significant difficulties and only few contributions have been proposed at the present on the topic (Pastor et al. 2004).

The objective of this paper is to propose an approach for the geomechanical modeling of failure and postfailure stages of these landslides and to show how different modeling alternatives, derived from the same mathematical framework, can be used to

[1]Full Professor, Dept. of Civil Engineering, Univ. of Salerno, Via Ponte Don Melillo, 1, 84084 Fisciano (SA), Italy.

[2]Assistant Professor, Dept. of Civil Engineering, Univ. of Salerno, Via Ponte Don Melillo, 1, 84084 Fisciano (SA), Italy (corresponding author). E-mail: scuomo@unisa.it

[3]Full Professor, ETS de Ingenieros de Caminos, Universidad Politécnica de Madrid, Ciudad Universitaria, s/n 28040 Madrid, Spain.

[4]Associate Professor, Dept. of Civil Engineering, Univ. of Salerno, Via Ponte Don Melillo, 1, 84084 Fisciano (SA), Italy.

Note. This manuscript was submitted on August 5, 2008; approved on June 18, 2009; published online on June 22, 2009. Discussion period open until June 1, 2010; separate discussions must be submitted for individual papers. This paper is part of the ***Journal of Geotechnical and Geoenvironmental Engineering***, Vol. 136, No. 1, January 1, 2010. ©ASCE, ISSN 1090-0241/2010/1-85–98/$25.00.

analyze one or both stages. To this aim, a literature review on the modeling of the failure and postfailure stages of flow-type landslides induced by rainfall infiltration is first provided. Then, an approach for the geomechanical modeling of the phenomena occurring inside the landslide source areas is presented and three different modeling alternatives are suggested highlighting the simplifications done to develop each one from the previous, from more to less complex. The potentialities of these models are then tested for a relevant case study from Southern Italy (Sarno-Quindici events, May 4–5, 1998). The obtained results are presented starting from the simplest model to the most complex, because it is the order usually followed in engineering when dealing with this type of problems. It will be shown how simple models provide results which are consistent with those of the more complex ones, outlining the effectiveness of the proposed approach.

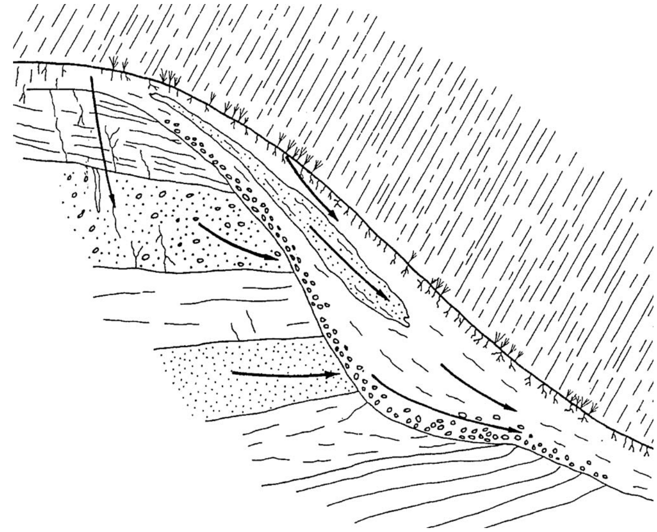

**Fig. 1.** Scheme of groundwater circulation inside shallow soil deposits and bedrock (after Johnson and Sitar 1990)

## Literature Review

### *Failure Stage*

The failure onset of rainfall-induced shallow landslides is strictly related to the increase of pore-water pressures and the consequent reduction of mean effective stresses (Anderson and Sitar 1995; Alonso et al. 1996; Iverson et al. 1997). According to Leroueil (2001), the failure stage of rainfall-induced shallow landslides of the flow-type in natural slopes is generally a drained process: that is, no variations of pore pressures are induced by the soil volume change. If the process can be assumed to develop under constant total normal stresses (Anderson and Sitar 1995; Take et al. 2004), the general in situ stress path can be described by a constant shear stress path associated to an increase of the effective stress ratio of the deviatoric stress $q$ to the effective mean stress $p'$.

Inside shallow soil deposits, the increase of pore-water pressures can be generated by rainfall (Fig. 1) that directly infiltrate the slope surface (Tsaparas et al. 2002; Futai et al. 2004) and propagate in depth through groundwater flow patterns related to stratigraphical setting of the slope (Ng and Shi 1998).

Sometimes pore-water pressure regime is also affected by the hydrogeological features of the underlying bedrock (Johnson and Sitar 1990; Montgomery et al. 1997; Matsushi et al. 2006) that can impose severe hydraulic boundary conditions at the bottom of the shallow deposits (Fig. 1). Typical examples are those of water table rising in the bedrock (Montgomery et al. 1997; Leroueil 2004) and/or by the presence of springs from the bedrock (Anderson and Sitar 1995; Anderson et al. 1997; Lacerda 2004; Onda et al. 2004).

The role played by bedrock groundwater flow in the triggering of landslides has been highlighted through in situ measurements and tests for colluvial deposits of the San Francisco Bay area (Johnson and Sitar 1990) and of the Oregon Coast Range (Anderson et al. 1997; Montgomery et al. 1997), as well as in unsaturated residual soil and completely decomposed granite of China (Zhang et al. 2000). Similarly, hydrogeological analyses (De Vita et al. 2006) coupled with geomorphological analyses (Cascini et al. 2000, 2008), have been used to highlight the importance of springs from the bedrock for shallow landsliding in pyroclastic deposits of southern Italy.

From the combination of rainfall that directly infiltrates the slope surface and spring from the bedrock a relevant triggering mechanism arises. For this triggering mechanism, current literature essentially provides the modeling of induced pore-water pressure regime (Calcaterra et al. 2004; Lacerda 2004; Matsushi et al. 2006) and few contributions deal with the slope stability conditions up to the failure onset (Cascini et al. 2000, 2003, 2005; Onda et al. 2004).

### *Postfailure Stage*

In the literature, the acceleration of the failed mass during the postfailure stage is attributed to different causes. However, most of the contributions identify as main cause the development of total or partial undrained conditions able to produce high pore-water pressures during shearing. In particular, for loose unsaturated soils, volumetric collapse is discussed by Olivares and Picarelli (2003), Yasufuku et al. (2005), Bilotta et al. (2006) and it is observed in constant-shear-drained triaxial tests upon wetting (Anderson and Riemer, 1995; Dai et al. 1999; Chu et al. 2003; Olivares and Damiano 2007). For loose saturated soils, static liquefaction is introduced by Wang et al. (2002), Olivares and Picarelli (2003), Van Asch et al. (2006) and observed in undrained triaxial tests (Lade 1992; Yamamuro and Lade 1998; Chu et al. 2003) as well as in undrained ring shear tests under controlled strain rates (Wang et al. 2002). Particularly, the build up of pore-pressures is shown to be relevant for soils having low density index (Eckersley 1990; Iverson 2000; Wang and Sassa 2001), fine grain size (Wang and Sassa 2003), low hydraulic conductivity (Iverson et al. 1997; Lourenco et al. 2006) and subjected to high deformation rate (Iverson et al. 1997).

Other contributions point out that the transition from slide to flow (Iverson et al. 1997; Take et al. 2004) is caused by local failures producing a variation in the slope geometry. This mechanism is related to transient localized pore-water pressures that are not associated to the development of undrained conditions, but originated from particular hydraulic boundary conditions and stratigraphical settings. Experimental evidences are available from centrifuge tests on small-scale slope models (Take et al. 2004) and small-scale flume tests (Lourenco et al. 2006) showing that the transition from slide to flow can occur both for loose and dense soils and can be associated to a decreasing in pore-water pressures during the postfailure stage.

Whatever the cause is, modeling of the postfailure stage is poorly addressed in the literature. The only available contributions refer to triggering factors that differ from rainfall, such as earthquake (Pastor et al. 2004) and kinematic or static perturbations (Laouafa and Darve 2002).

## Approach for Geomechanical Modeling

### *Remarks on Failure and Postfailure Stages*

In unsaturated shallow deposits, the triggering mechanism discussed in the "Failure Stage" section originates shallow landslides that can turn into landslides of the flow-type ("Postfailure Stage"). However, major differences can be outlined among slides, slides turning into flows and flowslides. In the following, a reference scheme is proposed (Fig. 2) that takes into account both direct rainfall infiltrating the slope surface and spring from bedrock. Particularly, Fig. 2 provides the effective stress paths in terms of the stress invariants $q$ and $p'$ defined as follows:

$$q = \frac{1}{\sqrt{2}}\sqrt{(\sigma_1' - \sigma_3')^2 + (\sigma_1' - \sigma_2')^2 + (\sigma_2' - \sigma_3')^2} \qquad (1)$$

$$p' = (\sigma_1' + \sigma_2' + \sigma_3')/3 \qquad (2)$$

The effective stress tensor $\sigma'$ has been taken as

$$\sigma' = \sigma - p_a I + S_r(p_a - p_w)I \qquad (3)$$

where $\sigma$=total stress tensor; $p_a$=air pore pressure; $p_w$=pore water pressure; $s=p_a-p_w$=suction; $S_r$; degree of saturation; and $I$ is the identity tensor of second order. In Fig. 2 the displacement ($\delta$), resisting force ($F_r$) and driving force ($F_d$) curves versus time are also shown.

For slides [Fig. 2(b)], soil mechanical behavior is controlled, in drained conditions, by the hydrologic response up to the failure onset. Resisting force ($F_r$) decreases up to the value of the driving force ($F_d$) along a slip surface that includes the zone where the spring from the bedrock is located (later named spring zone, Point A in Fig. 2) [Fig. 2(b), $t=t_1$]. Drained conditions also remain, both for loose and dense soils, during the postfailure stage and small accelerations develop [Fig. 2(b), $t>t_1$].

In loose saturated soils, the above process is associated with a volume reduction of the soil. If the pore-water pressure cannot freely dissipate, partially or totally undrained conditions develop during the Postfailure stage and a flowslide occurs [Fig. 2(d), $t>t_1$]. Particularly, in the spring zone (Point A in Fig. 2), pore-water pressures build up and the soil follows a stress path 0 to 1, leading to a catastrophic failure [Fig. 2(d), $t>t_1$]. In fact, the soil cannot sustain the imposed deviatoric stress $q$ thus accelerating along the stress path from 1 [Fig. 2(d), $t>t_1$].

Alternatively, slides can turn into flows [Fig. 2(c)] as a conse-

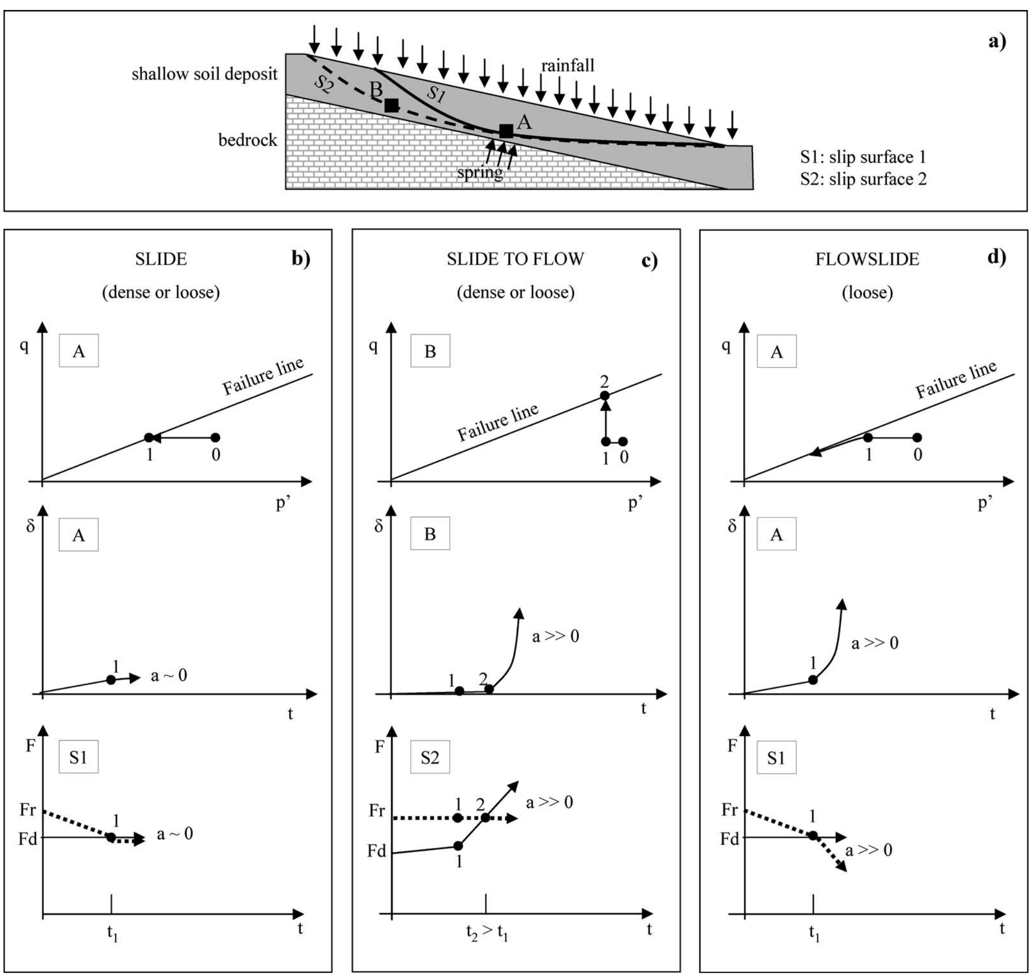


**Fig. 2.** Reference schemes adopted for the shallow landslides induced by rainfall directly infiltrating the slope surface and spring from the bedrock

quence of complex mechanisms characterized by a decreasing in the shear strength due to local hydraulic boundary conditions that can lead to fail the portion of the slope corresponding to the spring zone [Fig. 2(b) $t=t_1$]. Above this zone [Point B in Fig. 2], the mobilized shear stresses increase, both in loose and dense soils, due to the unbalanced driving forces along an upslope potential slip surface [Fig. 2(c), $t>t_1$] and a further slide can occur [Fig. 2(c), $t=t_2$]. The latter is characterized by a high initial acceleration and it consequently turns into a flow [Fig. 2(c), $t>t_2$].

Major differences between a flowslide [Fig. 2(d)] and a slide turning into flow [Fig. 2(c)] can be also outlined focusing on pore-water pressures at failure. For the analyzed schemes, pore-water pressures reach the highest values at Point A (spring zone) due to both rainfall and local hydraulic boundary conditions (i.e., spring from bedrock) and the lowest values at Point B (above the spring zone) being related only to the rainfall. Finally, the pore-water pressure values at failure can be negative at Point B [Fig. 2(c)] and slides turning into flow can also occur in portions of the slope characterized by unsaturated conditions.

Another important aspect to take into account is the type of failure. In the cases sketched in Figs. 2(b and c), drained failure takes place at the critical state line, and it can be of localized type (Pastor et al. 2002, 2004). On the contrary, fully or partially undrained postfailure stage of very loose materials [Fig. 2(d)] is of diffuse type (Darve and Laouafa 2000; Fernandez Merodo et al. 2004), and generation of pore-water pressures has to be carefully considered by using suitable constitutive and mathematical models. Notwithstanding the previous differences, it can be stated that for all the landslide typologies of Fig. 2, the eventual sudden acceleration of the failed mass (postfailures stage) is a consequence rather than a cause of the slope instability process, as experimentally demonstrated by Eckersley (1990) and Chu et al. (2003). This means that the failure and postfailure stages can be separately analyzed.

### *Mathematical Framework*

In order to properly reproduce the previously described typologies of shallow landslides, it is necessary to use: (i) a mathematical model describing the coupling between pore fluids and soil skeleton; (ii) a suitable constitutive relationship able to describe the unsaturated soil behavior; and (iii) a numerical model where (i) and (ii) are implemented. To the authors' knowledge, these have not been done yet in a full satisfactory manner, and until such tools are available, simplified models have to be carefully used. Hereafter, a mathematical framework is described mainly derived from the fundamental contributions of Zienkiewicz at al. (1980, 1999). This framework can be profitably used to simulate the landslide failure and postfailure stages.

It is assumed that the soil consists of a solid skeleton and two fluid phases, water and air, which fills the voids. The skeleton is made of particles of density $\rho_s$ with porosity $n$ (volume percent of voids in the mixture) and void ratio $e$ (volume of voids per unit volume of solid fraction).

Movement of the fluid is considered as composed of two parts, the movement of soil skeleton and motion of the pore water relative to it

$$v_w = v + w/n \tag{4}$$

where $v_w$=velocity of pore water and $w$=averaged velocity of water relative to the soil.

The total stress tensor $\sigma$ acting on the mixture can be decomposed into a hydrostatic pore pressure term $p_w I$ and an effective stress tensor $\sigma'$ acting on soil skeleton, which for unsaturated soils with zero air pressure is

$$\sigma = \sigma' - S_r p_w I \tag{5}$$

where $I$=second order identity tensor and tensile stresses are assumed as positive. Sometimes, the product $\bar{p}=S_r p_w$ is called averaged pore pressure.

The balance of momentum equation for the mixture can be written as

$$\mathrm{div}(\sigma' - \bar{p}I) + \rho b = \rho \frac{dv}{dt} \tag{6}$$

where the term $\rho_m n d/dt(w/n)$, which characterizes the acceleration of water relative to soil grains, is neglected. In above, $\rho$ is the mixture density, and $b$ the vector of body forces.

Concerning the balance of mass of the pore water, the following volume deformations $d\theta_i$ in the mixture are considered:

1. Deformation of soil skeleton

$$d\theta_1 = S_r\,\mathrm{tr}(d\varepsilon) = S_r d\varepsilon_v \tag{7}$$

where $d\varepsilon$=increment of the strain tensor; tr denotes the trace operator; and $d\varepsilon_v$=increment of volumetric strain.

2. Deformation of soil grains caused by pore pressure

$$d\theta_2 = \frac{1-n}{K_s} d\bar{p} = \frac{1-n}{K_s}\left(S_r + p_w \frac{C_s}{n}\right) dp_w \tag{8}$$

where $K_s$=volumetric stiffness of soil particles; and $C_s$ =specific moisture capacity.

3. Deformation of pore water caused by pore pressure

$$d\theta_3 = \frac{nS_r}{K_w} dp_w \tag{9}$$

where $K_w$=volumetric stiffness of pore water.

4. Increase of water storage

$$d\theta_4 = n dS_r = n \frac{\partial S_r}{\partial p_w} dp_w = C_s dp_w \tag{10}$$

From here, the mass conservation for the pore fluid can be written as

$$\mathrm{div}\ w + \frac{1}{Q^*}\frac{dp_w}{dt} + S_r\, tr\left(\frac{d\varepsilon}{dt}\right) + C_s \frac{\partial p_w}{\partial t} = 0 \tag{11}$$

where

$$\frac{1}{Q^*} = \left\{ \frac{nS_r}{K_w} + \frac{1-n}{K_s}\left(S_r + p_w \frac{C_s}{n}\right) \right\} \tag{12}$$

The balance of momentum of the pore fluid is

$$-\ \mathrm{grad}\ p_w + \rho_w b - \frac{1}{k_w} w = \rho_w \frac{dv}{dt} \tag{13}$$

where $\rho_w$=density of the water and $k_w$=hydraulic conductivity. The Darcy law can be used to describe the interaction between pore water and soil skeleton, although other alternatives can be chosen. In above, the accelerations of the pore water relative to soil skeleton are neglected.

Balance of mass and momentum of the pore fluid can be combined by substituting the value of $w$ given by the latter into the former, arriving to

$$\left(C_s+\frac{1}{Q^*}\right)\frac{dp_w}{dt}+S_r\,\mathrm{div}\,v-\mathrm{div}(k_w\,\mathrm{grad}\,p_w)=0 \qquad (14)$$

where the term $\mathrm{div}(-\rho_w b+\rho_w dv/dt)$ is neglected in geotechnical analysis, because body forces are independent of space coordinates (with the exception of scale centrifugal tests), and the space derivatives of accelerations are assumed to be small.

Eqs. (6) and (14) have to be complemented by a kinematic relation linking velocities to rate of deformation tensor, and a suitable constitutive or rheological equation.

### *Modeling Alternatives*

The coupled stress-strain model described in the previous paragraph have been recently used for simulating the failure stage of earthquake-induced landslides of the flow-type (Fernandez Merodo et al. 2004; Pastor et al. 2004) and for the propagation stage of rainfall-induced landslides of the flow-type (Pastor et al. 2008). Indeed, it could be profitably used for the simulation of the failure and postfailure stages of all the landslide typologies sketched in Fig. 2. However, advanced constitutive models have to be used to reproduce postfailure phenomena such as liquefaction (Sladen et al. 1985; Chu et al. 2003) and instability phenomena (Darve and Laouafa 2000). Since the failure and postfailure stages of the landslides sketched in Fig. 2 can be separately addressed, simplified versions of this model can be usefully derived, aimed to their application in case only the failure stage is of concern.

Within the mathematical framework of "Mathematical Framework" section, an uncoupled stress-strain model can be obtained based on simplifying assumptions. Particularly, if the deformation rate can be neglected without appreciable errors and if water and grain compressibility are assumed as negligible, Eq. (14) finally reduces to the well-known equation of Richards (1931) [Eq. (15)] from which pore-water pressures $p_w$ can be computed. From Eq. (6), neglecting the deformation rate, we obtain Eq. (16), from which stresses $\sigma'$ can be computed based on known pore-water pressures $p_w$. Finally, deformations and displacements are computed through a suitable constitutive equation and the kinematic relation

$$C_s\frac{d\bar{p}}{dt}-\mathrm{div}(k_w\,\mathrm{grad}\,\bar{p})=0 \qquad (15)$$

$$\mathrm{div}(\sigma'-\bar{p}I)+\rho b=0 \qquad (16)$$

In the above equations, the averaged pore pressure $\bar{p}$ influences the mechanical behavior but, in turn, the latter does not influence the former. Consequently, if drained conditions are assumed, the uncoupled model can be usefully applied for the simulation of the failure stages of both slides [Fig. 2(b)] and slides turning into flows [Fig. 2(c)].

Finally, classical limit equilibrium models can be considered as a last modeling alternative derived from the mathematical framework of "Mathematical Framework" section. As in the case of the uncoupled stress-strain model, these models can be applied for the failure stage of rainfall-induced landslides since rainfall modifies the pore-water pressures in drained conditions and deformation rate (i.e., acceleration of soil mass) can be surely neglected. As main advantage, this model only requires soil unit weight and soil shear strength as input data. Of course, pore pressures have to be taken into account, but Eq. (6) is substituted by an integral form obtained from its integral in volume

$$\int_\Omega \mathrm{div}(\sigma'-\bar{p}I)d\Omega+\int_\Omega \rho b d\Omega=0 \qquad (17)$$

from where, applying Gauss theorem, it derives that

$$\int_\Gamma (\sigma'-\bar{p}I)\,.\,nd\Gamma=\int_\Omega \rho b d\Omega \qquad (18)$$

where the integral on the boundary $\Gamma$ is evaluated assuming that the stress state is on the failure surface. In above, $n$ is the normal to the domain.

In the practice, considering a potential unstable soil mass (i.e., defined assuming a potential slip surface) and dividing it into vertical slices, Eq. (18) reduces to the basic equations of the limit equilibrium methods. However, based on Eqs. (15) and (18) the problem is indeterminate and different hypotheses have been proposed to represent the internal forces [Janbu (1954), Bishop (1955), Morgenstern and Price (1965), among others]. In limit equilibrium analyses, the factor of safety (FS) is considered. It is generally defined as the ratio of the shear strength of soil to the minimum shear strength required for equilibrium (Bishop 1955) or, alternatively, as the minimum factor by which the soil shear strength would have to be divided to bring to failure (Duncan 1996). Moreover, the potential slip surfaces are assumed as input data and they require careful evaluations on their shape and location eventually through optimization techniques (Duncan 1996; Malkawi et al. 2001).

In conclusion, the selection among the previous modeling alternatives (coupled stress-strain, uncoupled stress-strain and limit equilibrium models) must be based on the addressed issue (failure stage or failure and postfailure stages), and other relevant aspects such as, for instance, the scale of the analysis and the available data set. Anyway, the integrated use of different models is strongly recommended in order to capture the essential aspects of complex real boundary value problems, so obtaining significant answers from an engineering point of view.

## Case Study

In order to check the usefulness of the presented geomechanical approach and the potentialities of the above-described modeling alternatives, it is worthwhile to test these models for a well-documented case history. A significant example is provided by the landslides of the flow-type occurred in May 1998 in pyroclastic deposits of the Campania region (southern Italy). For this case, geological, geomorphological, hydrogeological and geotechnical high quality data sets are available for the landslides characterization and analysis.

### *General Features of the May 4–5, 1998 Event in Campania Region*

The event addressed in this section occurred on May 4–5, 1998 when, in about 16 h, more than 100 shallow landslides were triggered by rainfall along the slopes of the Pizzo d'Alvano carbonate massif (Cascini 2004; Cascini et al. 2008). Tens of these shallow landslides turned into catastrophic landslides of the flow-type (Fig. 3) and traveled downslope from the source areas up to distances greater than 2 km (Revellino et al. 2004). They caused relevant property damage and loss of human life (159 victims) in the four towns located at the toe of the massif.

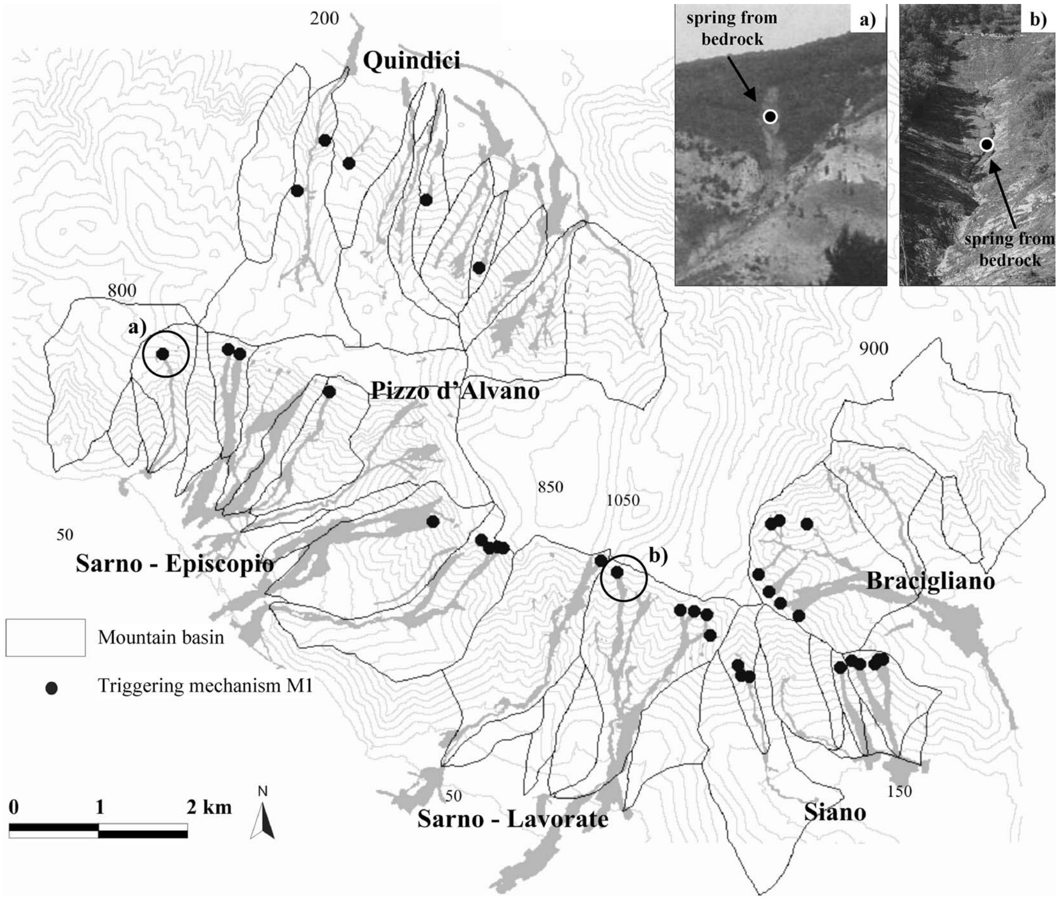


**Fig. 3.** Overview of the landslides of the flow-type occurred in May 1998

During this event, over a 48 h period, a cumulated rainfall equal to 120 mm was measured by the rain gauges located at the toe of the Pizzo d'Alvano massif (Cascini et al. 2000; Cascini 2004; Fiorillo and Wilson 2004). However, after May 1998, rain gauges were also installed at the top of the massif. Here, during 1–2 day rainstorms, rainfall values are frequently higher (1.5–2.0 times) than those recorded at the toe of the slopes. Based on these results, it can be reasonably argued that, also on May 4–5, 1998, the cumulated rainfall was higher than that measured at the toe of the massif (Cascini et al. 2003).

Many contributions deal with the failure and postfailure stage of these landslides as summarized by Cascini et al. (2005, 2008) and Cuomo (2006). Particularly, these Authors recognize six typical triggering mechanisms by concurrently taking into account the location of the landslides source areas, the geomorphological and hydrogeological features of the massif, as well as the anthropogenic factors. The combination of these factors was related to the occurrence of slope failures and to the characteristics of the landslides source areas (Cascini et al. 2008).

Among these typical triggering mechanisms, the most frequent one (named M1 and the 28% over a total of 133 analyzed landslides source areas) was the triggering mechanism described in "Remarks on Failure and Postfailure Stages" section (Fig. 2). According to Cascini et al. (2008), this mechanism occurred inside colluvial hollows, i.e., the so-called Zero Order Basins (Dietrich et al. 1986; Cascini et al. 2000; Guida 2003), which are characterized by convergent groundwater circulation inside the pyroclastic deposits and temporary springs from the bedrock (Fig. 3).

### *Available Data Set*

The geomechanical models described in "Modeling Alternatives" section require accurate information on stratigraphy, pore-water pressures, mechanical soil properties to be acquired through in situ and laboratory investigations (Fig. 4).

Referring to the analyzed case study, the in situ investigations (i.e., pits, seismic prospections and soil suction measurements collected over the period 1998–2004) provide detailed stratigra-

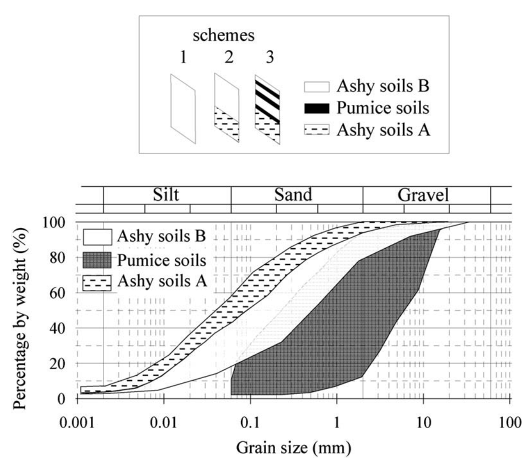


**Fig. 4.** In situ conditions and granulometric soil properties

**Table 1.** Physical and Mechanical Properties Assumed for the Pyroclastic Soils

| | $\gamma_d$ (kN/m$^3$) | $\gamma_{sat}$ (kN/m$^3$) | $n$ (−) | $k_{sat}$ (m/s) | $c'$ (kPa) | $\varphi'$ (°) | $\varphi^b$ (°) | $\nu$ (−) | $E$ (kPa) | $\psi$ (°) |
|---|---|---|---|---|---|---|---|---|---|---|
| Ashy soils (Class A) | 9.10 | 15.7 | 0.66 | $10^{-6}$ | 5÷15 | 32÷35 | 20 | — | — | — |
| Pumice soils | 6.20 | 13.1 | 0.69 | $10^{-4}$ | 0 | 37 | 20 | — | — | — |
| Ashy soils (Class B) | 7.30 | 13.1 | 0.58 | $10^{-5}$ | 0÷5 | 36÷41 | 20 | 0.29 | 3,000÷7,000 | 0÷20 |

Note: $\gamma_d$=dry unit weight; $\gamma_{sat}$=saturated unit weight; $n$=porosity; $k_{sat}$=saturated hydraulic conductivity; $c'$=effective cohesion; $\varphi'$=friction angle; and $\varphi^b$=rate of increase in shear strength due to suction.

phy of the pyroclastic deposits at site and massif scales (1:2,000–1:5,000), as well as soil suction regime during the hydrological year all over the Pizzo d'Alvano massif, inside and near the landslides source areas (Cascini and Sorbino 2002; Cascini 2004; Sorbino 2005).

As it concerns the laboratory investigations, they provide the physical and mechanical properties of the pyroclastic soils in both saturated and unsaturated conditions. Particularly, the pyroclastic deposits are essentially made up of pumice soils and two main classes (A and B) of ashy soil layers. The soil water characteristic curves for both the ashy soils obtained through the suction controlled oedometer, the volumetric pressure plate extractor and the Richard pressure plate are discussed by Sorbino and Foresta (2002). For the pumice soils, empirical relationships were used for the volumetric water content and the hydraulic conductivity curves (Sorbino and Foresta 2002; Bilotta et al. 2005). Finally, the shear strength and the compressibility properties of the involved soils in both saturated and unsaturated conditions are presented and discussed by Bilotta et al. (2005, 2006, 2008).

The main geotechnical parameters provided by the laboratory tests are summarized in Table 1 that also takes into account the data provided by the literature for analogous soils (Crosta and Dal Negro 2003; Calcaterra et al. 2004; Picarelli et al. 2004; Bilotta et al. 2005, 2006, 2008).

## Geomechanical Modeling

The analysis of the triggering mechanism named M1 was performed through an integrated use of the geomechanical models of "Modeling Alternatives" section (limit equilibrium, uncoupled stress-strain, and coupled stress-strain models). Particularly, limit equilibrium analyses were used at site scale to back-analyze the failure stage of a single landslide. To this aim, a detailed slope section was referred to assess the relevant factors leading to failure. Once these factors have been outlined, limit equilibrium analyses were also carried out at massif scale in order to check the significance of these factors for the attainment of failure conditions all over the Pizzo d'Alvano massif. The analyses at massif scale necessarily took into account simplified slope models that average the different site stratigraphy and slope geometry. Uncoupled and coupled stress-strain analyses were also performed at massif scale in order to validate the previous results and to get insights on the postfailure stage.

### *Limit Equilibrium Analyses*

For the analysis at site scale, a detailed slope section (Fig. 5) was examined. The geomechanical analyses primarily concerned the modeling of pore-water pressure changes during the time period from January 1, 1998 to May 5, 1998. Pore-water pressures were computed with a saturated-unsaturated groundwater modeling with the aid of the commercial finite element code SEEP/W (Geoslope 2005) that integrates Eq. (15). The soil parameters of Table 1 were used. The adopted FEM mesh resulted in 3,755 quadrilateral elements with lengths and heights respectively smaller than 1.0 and 0.5 m. As initial conditions, suction values were assumed respectively equal to 5, 10, 15, and 20 kPa, all over the slope section. A flux boundary condition equal to daily rainfall intensities recorded at the toe rain gauges was assumed on the ground surface for the period January 1, 1998—May 3, 1998; for the last two days (May 4–5) the flux boundary condition was, instead, assigned hourly rainfall intensities, with values equal to twice those recorded at the toe rain gauges. Evapotranspiration phenomena were not taken into account, according to Sorbino (2005), who evidenced the negligible effects of such phenomena in the modeling of suction regime during the spring season. At the contact between the pyroclastic deposit and the limestone bedrock, an impervious condition was assumed except for the zone where the spring from the bedrock is located (Fig. 5). Here, a flux condition was considered with a flux value of $1.67\times10^{-5}$ m$^3$/s, starting from May 2 or 3, 1998.

The results from seepage analyses point out that direct rainfall infiltration from ground surface and spring from the bedrock induce, at site scale, complex transient unsaturated-saturated flow patterns, strongly dependent on: (i) local stratigraphy; (ii) initial conditions; (iii) hydraulic boundary conditions. Fig. 6 shows, for instance, the role played by local stratigraphy and hydraulic boundary conditions on the computed pore-water pressures. It is worth noting that other Authors stress the role played by local stratigraphy on pore-water pressure regime in different geological contexts. Particularly, Ng and Shi (1998), Crosta and Dal Negro

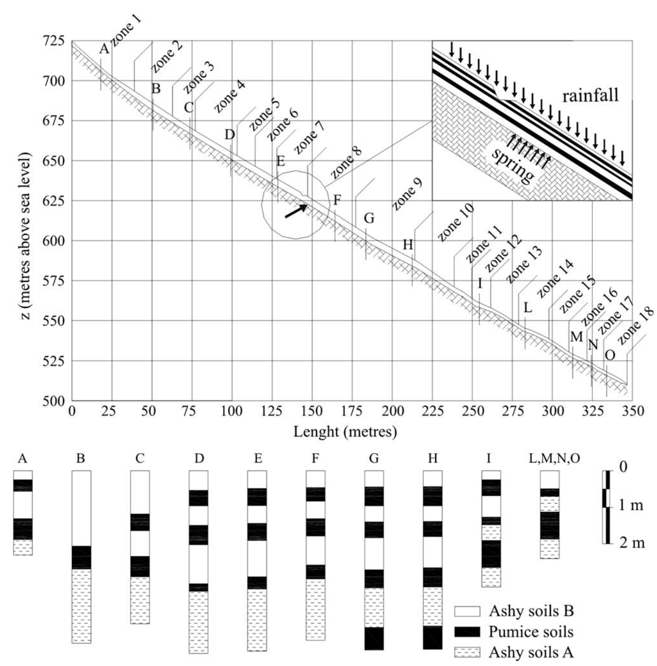


**Fig. 5.** Stratigraphy for limit equilibrium analyses at site scale

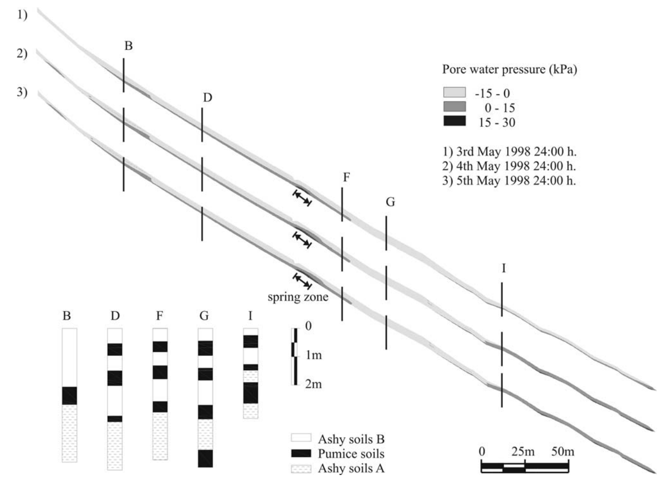


**Fig. 6.** Simulated pore-water pressures for the slope section of Fig. 5, assuming 10 kPa as initial conditions on January 1, 1998 and the spring starting from May 2, 1998

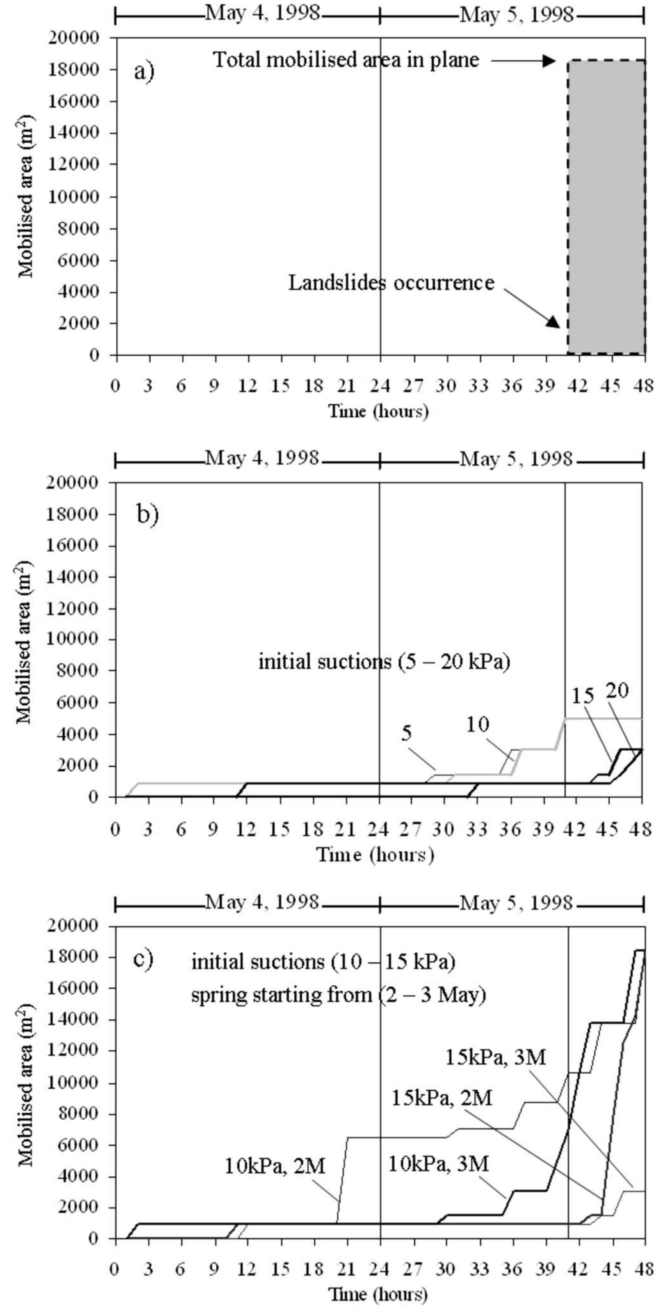


**Fig. 7.** Slope failure time sequence simulated for the slope section of Fig. 5

(2003) and Cascini et al. (2005) focus on the effects of local variations of geometry, while Reid (1997) and Lourenco et al. (2006) stress the relevance of differences in soil layers hydraulic conductivity. The initial conditions (i.e., saturation degree and water content), that determine the initial hydraulic conductivity, are considered also in the literature a key factor and they are demonstrated to be related to antecedent rainfall (Tsaparas et al. 2002) and/or to seasonal changes of suction (Blight 1997; Cascini and Sorbino 2002; Cascini et al. 2003). Hydrological seasons also determine different hydraulic boundary conditions at ground surface (i.e., rainfall) and bedrock contact (i.e., spring from bedrock) that, in turn, cause different pore-water regimes and available soil shear strength along the slip surface (Fredlund et al. 1978).

Using the computed pore pressures values, slope stability conditions were evaluated by integrating Eq. (18). To this aim, the limit equilibrium methods proposed by Janbu (1954) and Morgenstern and Price (1965) were adopted and the corresponding FS values were computed by using the commercial SLOPE/W code (Geoslope 2005). For all the involved soils, a rigid-perfectly plastic constitutive model was referred considering, in both saturated and unsaturated conditions, the extended Mohr-Coulomb failure criterion proposed by Fredlund et al. (1978) with geotechnical properties listed in Table 1. A full parametric analysis was performed changing initial suction and hydraulic boundary conditions in order to obtain a satisfactory fitting among the failure time sequence and the available eyewitnesses. In particular, at time steps ranging from 1 to 0.25 h, the FS were computed along 170 potential slip surfaces with different lengths and depth from the ground surface. When failure conditions (i.e., FS=1) were simulated at some portions of the slope, the stratigraphical slope section was updated removing the failed portions and slope stability conditions were recomputed for the remaining portions of the slope section. Slope stability analyses allow well reproducing the observed slope instability phenomena. Particularly, the analyses highlight that multiple slides are simulated along the slope according to a complex time sequence (Fig. 7), which is strictly dependent on suction initial conditions, as well as to the presence and starting time of the spring from the bedrock (Cascini et al. 2005, 2008). According to the scheme of Fig. 2, in the spring zone and upslope, retrogressive multiple slides are simulated, in drained conditions, taking into account the change of slope geometry, in agreement with the results provided by Take et al. (2004) and Ng (2008) for slope model centrifuge tests.

Once the most relevant factors affecting the failure stage of a single slope have been defined, limit equilibrium analyses were performed at massif scale, to check the validity of the model at more general site conditions. To this aim, infinite slope schemes were referred and parametric analyses were performed with typical slope angles (35°), depths (4.5 m) and stratigraphical settings (Fig. 8) provided by the in situ evidences (Cascini 2004). Particularly, the scheme 3 well averages the stratigraphy of the slope section of Fig. 5, while the scheme 2 and 1 are representative of other portions of the Pizzo d'Alvano massif. The same soil properties, initial and hydraulic boundary conditions of site scale

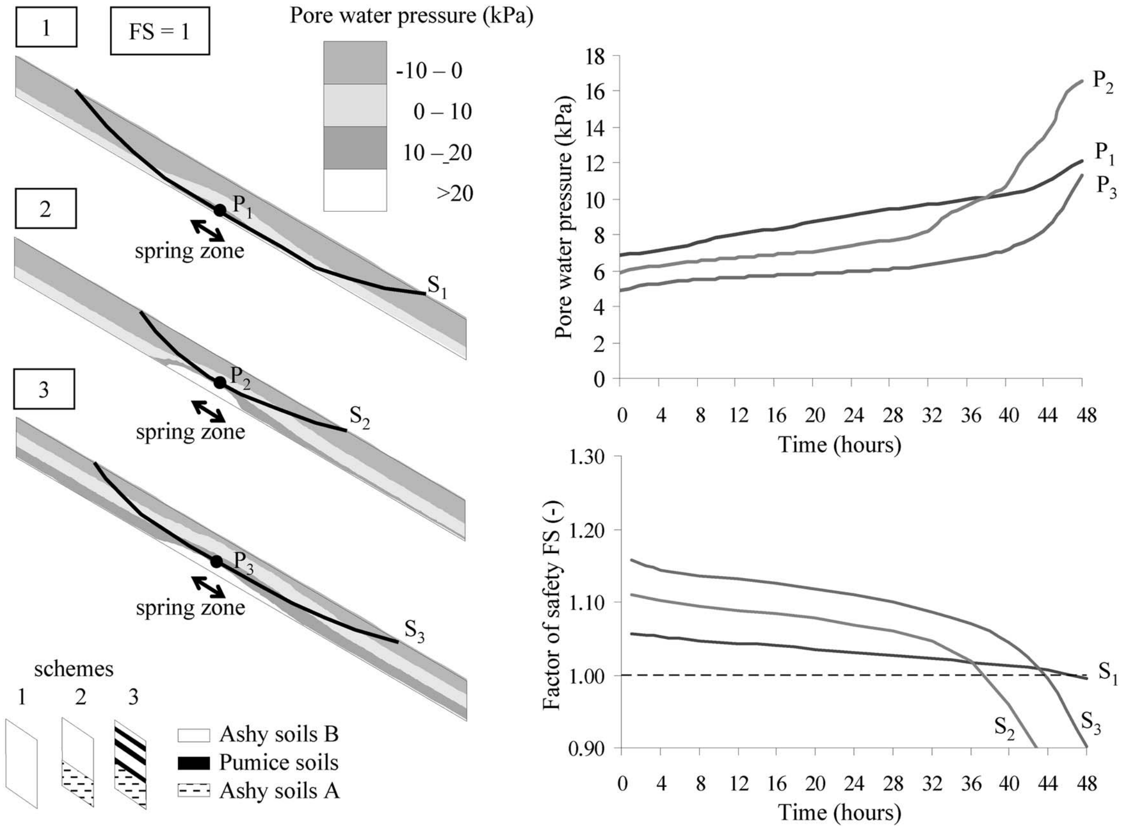


**Fig. 8.** Limit equilibrium analyses at massif scale: pore-water pressures and slope FS

analyses were adopted. The numerical results of the parametric analysis (Fig. 8) indicate that rainfall infiltration from ground surface and spring from the bedrock increase the pore-water pressures up to the slide occurrence [Fig. 2(b)], independently from the assumed stratigraphical setting and for any shear strength value listed in Table 1 (Cascini et al. 2005). Different stratigraphical settings and mechanical properties of pyroclastic deposits only determine different depths of the slip surfaces from the ground surface (Cascini et al. 2005).

In conclusion, the obtained results show that localized pore-water pressures, induced by spring from bedrock, must be confirmed as the key factor for the failure onset also at massif scale. This is clearly pointed out by the correlation between the maximum pore-water pressures along the critical slip surfaces and their factors of safety (points $P_1$-$P_3$ along slip surfaces $S_1$-$S_3$ in Fig. 8). The time of simulated failures also well fit the in situ eyewitnesses (Fig. 8).

### *Uncoupled Stress-Strain Analyses*

More detailed information and further insights on the failure stage can be obtained through uncoupled stress-strain analyses. These analyses were performed through the commercial finite element SIGMA/W code (Geoslope 2005) that integrates the Eq. (16). This code uses as input data the pore-water pressures provided by the SEEP/W code (Geoslope 2005) through the integration of Eq. (15). Taking into account the previous results showing the small influence of the particular stratigraphical setting on the failure occurrence, the analyses were carried out referring to the simplest infinite slope scheme of Fig. 8 (i.e., scheme 3, containing only ashy B soils) and to the period May 4–5, 1998. For both the SEEP/W and SIGMA/W analyses, the previous finite element meshes were used, adopting an elastoplastic constitutive model with a Mohr-Coulomb criterion extended to unsaturated conditions (Fredlund et al. 1978), whose parameters are summarized in Table 1. As it concerns the hydraulic boundary conditions, a constant rainfall intensity was considered with a cumulated value equal to that used in the previous analyses and a spring zone was introduced with different flux values, ranging from $4.17 \times 10^{-6}$ to $1.67 \times 10^{-5}$ $m^3/s$. Simplified initial conditions were assumed at May 4, 1998, i.e., a uniform distribution of suction equal to 5 kPa that well fits the pore-water pressures simulated with a full seepage analysis for the period January 1–May 3 1998. The initial stress field was evaluated by simulating the deposition process of the pyroclastic materials with a multistep increase of the soil deposit's depth.

Using the previous described schemes, a parametric analysis was performed changing the flux values of the spring and soil properties among those reported in Table 1. The obtained results highlight that, disregarding the spring from the bedrock, rainfall infiltration from the ground surface induces low deformation rates in the slope and the observed failure onset cannot be simulated. On the contrary, by considering the spring from bedrock, higher pore-water pressures, stress ratios and deformation rates are simulated in the portion of the slope corresponding to the spring zone, in agreement with the limit equilibrium analyses shown in Fig. 8 and accordingly to the scheme of Fig. 2(b). Particularly, Fig. 9 shows the results obtained for the scheme 1 of Fig. 8, assuming the spring from bedrock starting from 4 May 1998 with a flux value of $1.67 \times 10^{-5}$ $m^3/s$. In such a case, displacements are induced in the spring zone (Points $A_1$ and $A_2$) by the reduction of effective mean stress $p'$ at nearly constant deviatoric stress $q$ (Fig. 9), and the occurrence of a slide in drained conditions is clearly

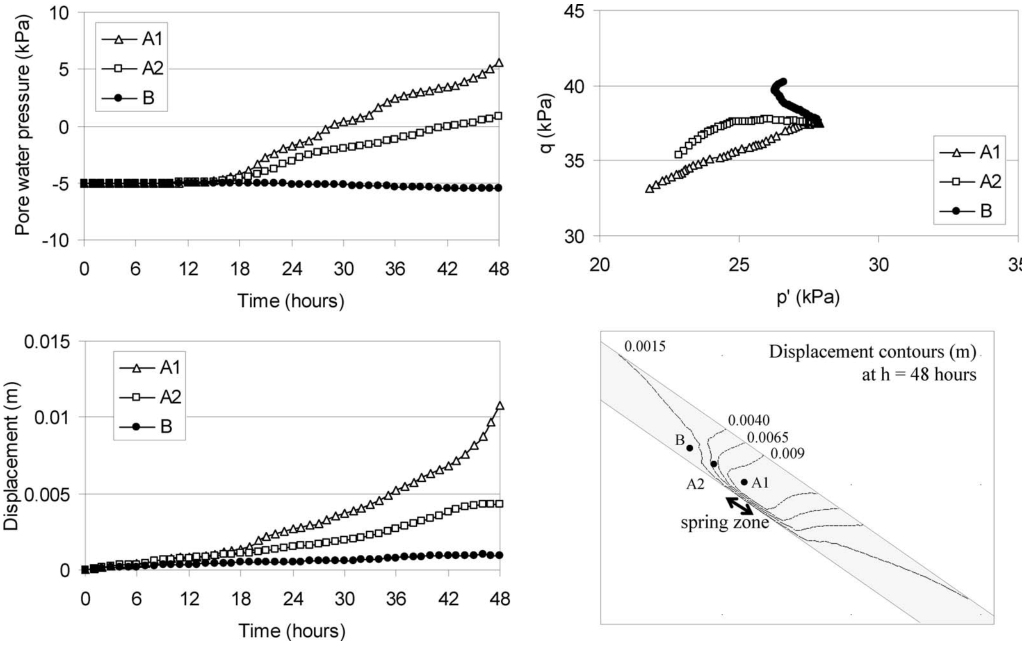


**Fig. 9.** Uncoupled stress-strain analyses at massif scale: pore-water pressures, displacements, and stress paths for the Scheme 1 of Fig. 8

outlined. In the upslope zone (Point B) a different stress path in the $q-p'$ plane is simulated as well as a different time trends for pore-water pressures and displacements, in agreement with the scheme of Fig. 2(c). In this zone the displacements are induced by the failure onset at the spring zone, and they are related to the increase of deviatoric stress $q$ at nearly constant effective mean stress $p'$ (Fig. 9). This process corresponds to the initial stage of a further slide that can turn into a flow as shown by Take et al. (2004) and Ng (2008). However, this process is not completely simulated being not available a numerical model automatically updating the slope geometry. Notwithstanding these limitations and the simplified hypotheses, it is worth noting that the simulated displacements field (Fig. 9) matches well the failed masses assessed through limit equilibrium analyses (Fig. 8). Moreover, the time failure agrees the in situ eyewitnesses as well as those obtained with limit equilibrium analyses (Fig. 8). Similar results were obtained for different values of the soil Young modulus $E$ and the dilation angle $\Psi$ among those listed in Table 1. Particularly, the simulated displacements slightly increase by decreasing the $E$ modulus while the dilation angle $\Psi$ plays a negligible role. Moreover, the simulated stress paths are practically independent from both the $E$ and $\Psi$ values.

### Coupled Stress-Strain Analyses

The modeling of both failure and postfailure stages was finally addressed through coupled stress-strain analyses at massif scale, using the GeHoMadrid code (Mira McWilliams 2002). This code concurrently integrates Eqs. (6) and (14), so providing pore-water pressures dependent on both hydraulic boundary conditions and soil compressibility behavior, as well as the stress and strain fields.

An infinite slope scheme and the stratigraphy of the scheme 1 of Fig. 8 were used for the analyses, considering the same initial and hydraulic boundary conditions as well as the same simple constitutive model (Table 1) of "Uncoupled Stress-Strain Analyses" section. The results obtained for $E=3000$ kPa and $\Psi=20°$ (Fig. 10) confirm that significant plastic strains are simulated only if both rainfall and spring from the bedrock are considered. Moreover, the simulated slope instability scenario and the time failure well agree those obtained with the previous simplified analyses (i.e., limit equilibrium and uncoupled stress-strain analyses) (Figs. 8 and 9), thus highlighting their capability to capture the global behavior of the slope. Moreover, a parametric analysis, with different values of the soil Young modulus $E$ and the dilation angle

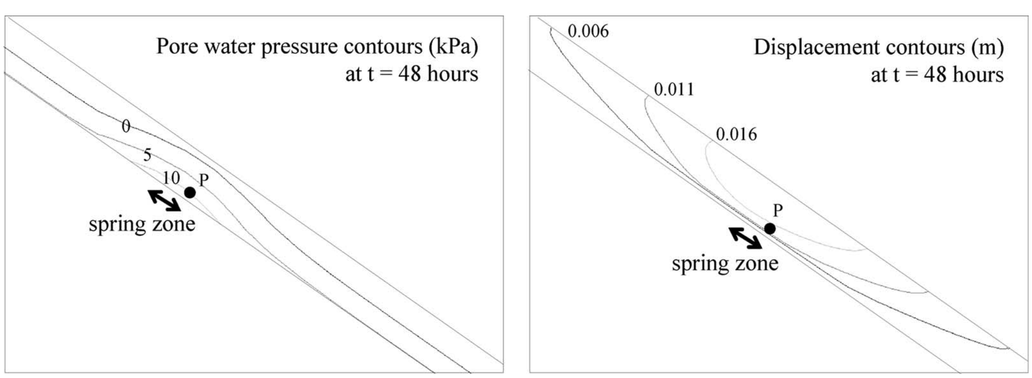


**Fig. 10.** Coupled stress-strain analyses at massif scale: pore-water pressures and displacement contours

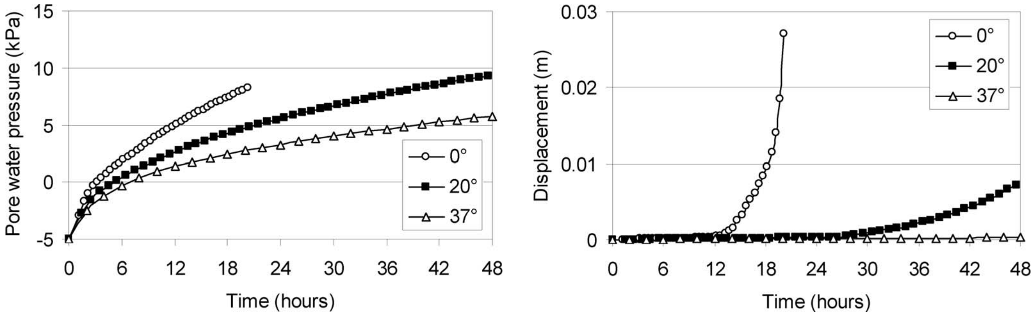


**Fig. 11.** Pore-water pressures computed through the coupled model for the point $P$ of Fig. 10

$\Psi$ among those listed in Table 1, highlight that the numerical results slightly depend on the parameter $E$. Conversely, the dilation angle $\Psi$ plays an important role, affecting both the computed pore-water pressures and displacements (Fig. 11). Particularly, (i) the highest values and gradients of pore-water pressures and displacements are simulated for a value of the dilation angle $\Psi$ equal to 0° (i.e., not associated flow rule), while (ii) the failure onset cannot be simulated and the computed displacements are negligible for a value of the dilation angle $\Psi$ equal to 37° (i.e., associated flow rule).

As for the postfailure stage, the obtained results allow to outline some remarks, taking into account the simple constitutive model used. Particularly, (i) significant differences in pore-water pressures are simulated in the spring zone by only changing the dilation $\Psi$ (Fig. 11); (ii) depending on $\Psi$ value, the build up of high pore-water pressures can be highlighted and the possible occurrence of static liquefaction can be argued, in agreement with the scheme of Fig. 2(d). Therefore, the coupling between pore-water and solid skeleton plays an important role and the deformation mechanism strictly affects the landslide failure and postfailure stages. However, only when a suitable constitutive model is available, it will be possible to distinguish between the occurrence of a slide [Fig. 2(b)] or a flowslide [Fig. 2(d)] in the spring zone.

As commonly accepted in the practice, all the previous analyses were based on the assumption of plain strains conditions along the considered longitudinal slope section. Removing this hypothesis, the coupled stress-strain analyses were finally extended to three-dimensional (3D) conditions, to check the validity of the previous results. A 3D slope characterized by a concave transversal bedrock profile and a variable depth for the overlying pyroclastic deposit (ranging between 4.5 and 2 m, with the maximum value corresponding to the central part of the concavity) was considered. The previous soil properties as well as initial and hydraulic boundary conditions were used. Particularly, the presence of a spring from bedrock was assumed in the central part of the concavity (spring zone).

The obtained results highlight that rainfall and spring from the bedrock induce high local pore-water pressures in the spring zone where the highest stress ratios, plastic strains and displacements were computed (Fig. 12). The simulated landslide source area is characterized by an elongated platform not laterally enlarging. It is worth noting that the 3D coupled analyses agree with the slope instability scenarios obtained through two-dimensional (2D) coupled analyses and they well match the results obtained with simplified models (Figs. 8–10). Moreover, the 3D coupled analyses provide a landside source area that well matches the in situ observations and geomorphological evidences (Fig. 3, Section 4). Hence, 3D effects are outlined as negligible, and more conventional 2D analyses can be safely referred.

## Conclusions

Landslides of the flow-type are frequently triggered by rainfall in shallow soil deposits. The failure stage is mainly associated to rainfall that directly infiltrate the slope surface and to spring from

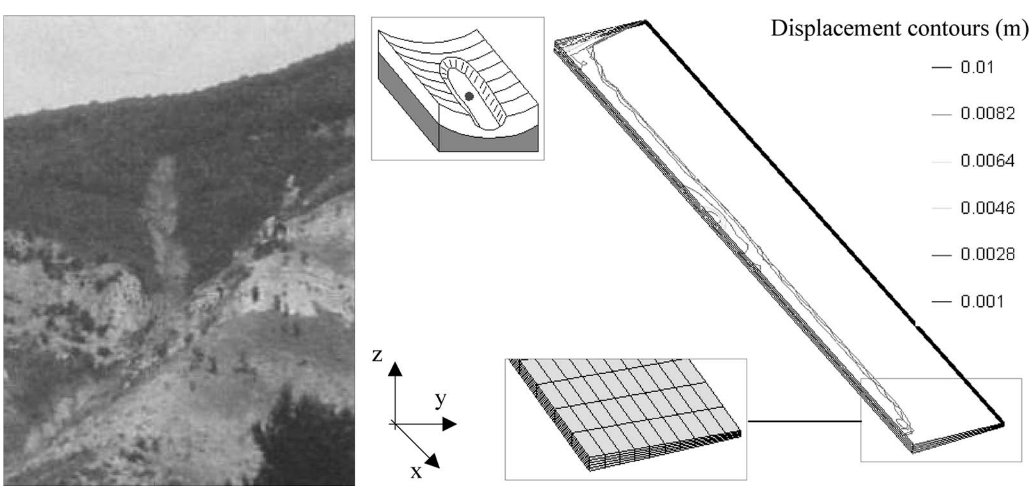


**Fig. 12.** 3D coupled stress-strain analyses: displacement contours

the underlying bedrock. The postfailure stage is characterized by the sudden acceleration of the failed mass. Based on the current literature, some reference schemes for the analysis of these landslides have been adopted. Then, assuming that failure and postfailure stages can be separately addressed, an approach for the geomechanical modeling is presented and three different modeling alternatives are suggested to analyze one or both stages at different scales. Numerical analyses are finally provided for a well-documented case history of southern Italy (Sarno-Quindici event, May 4–5, 1998).

For this case history, simple limit equilibrium analyses point out, at site scale, the role played by local stratigraphy, initial and hydraulic boundary conditions as predisposing and triggering factors of multiple slides characterized by a complex failure time sequence. At massif scale, limit equilibrium and 2D uncoupled stress-strain analyses confirm the role of rainfall infiltration and springs from bedrock as key factors for the failure stage. More sophisticated coupled 2D and 3D stress-strain analyses validate the previous results for the failure stage and provide insights on the postfailure stage and the landslide failing volume. In conclusion, the performed analyses clearly highlight the occurrence of a slide due to rainfall infiltration and spring from bedrock and the potential for this slide in turning into flow because of the deformation mechanism. This last aspect, however, will be properly addressed only when a suitable constitutive model is available.

## References


Alonso, E., Gens, A., Lloret, A., and Delahaye, C. (1996). "Effect of rain infiltration on the stability of slopes." *Proc., Int. Conf. on Unsaturated Soils*, E. E. Alonso and P. Delage, eds., Balkema, Rotterdam, 241–249.

Anderson, A., and Sitar, N. (1995). "Analysis of rainfall-induced debris flow." *J. Geotech. Engrg.*, 121(7), 544–552.

Anderson, S. A., and Riemer, M. F. (1995). "Collapse of saturated soil due to reduction in confinement." *J. Geotech. Engrg.*, 121(2), 216–220.

Anderson, S. P., Dietrich, W. E., and Montgomery, D. R. (1997). "Subsurface flow paths in a steep, unchanneled catchment." *Water Resour. Res.*, 33(12), 2637–2653.

Bilotta, E., Cascini, L., Foresta, V., and Sorbino, G. (2005). "Geotechnical characterization of pyroclastic soils involved in huge flowslides." *Geotech. Geolog. Eng.*, 23, 365–402.

Bilotta, E., Foresta, V., and Migliaro, G. (2006). "Suction controlled laboratory tests on undisturbed pyroclastic soil: Stiffnesses and volumetric deformations." *Proc., Int. Conf. on Unsaturated Soils*, Vol. 1, Carefree, Arizona, 849–860.

Bilotta, E., Foresta, V., and Migliaro, G. (2008). "The influence of suction on stiffness, shear strength, viscosity and collapse of some volcanic ashy soils." *Proc., European Conf. on Unsaturated Soils*, Durham, U.K., 349–354.

Bishop, A. W. (1955). "The use of the slip circle in the stability analysis of slopes." *Geotechnique*, 5(1), 7–17.

Blight, G. E. (1997). "Interactions between the atmosphere and the Earth." *Geotechnique*, 478(4), 715–767.

Calcaterra, D., de Riso, R., Evangelista, A., Nicotera, M. V., Santo, A., and Scotto di Santolo, A. (2004). "Slope instabilities in the pyroclastic deposits of the carbonate Apenine and the phlegrean district (Campania, Italy)." *Proc., Int. Workshop "Flows 2003—Occurrence and Mechanisms of Flows in Natural Slopes and Earthfill*, L. Picarelli, ed., Patron, Balogna, 61–75.

Capra, L., Lugo-Hubp, J., and Borselli, L. (2003). "Mass movements in tropical volcanic terrains: the case of Teziùtlan (Mexico)." *Eng. Geol. (Amsterdam)*, 69, 359–379.

Cascini, L. (2004). "The flowslides of May 1998 in the Campania region, Italy: the scientific emergency management." *Italian Geotechnical Journal*, 2, 11–44.

Cascini, L., Cuomo, S., and Guida, D. (2008). "Typical source areas of May 1998 flow-like mass movements in the Campania region, Southern Italy." *Eng. Geol. (Amsterdam)*, 96, 107–125.

Cascini, L., Cuomo, S., and Sorbino, G. (2005). "Flow-like mass movements in pyroclastic soils: remarks on the modelling of triggering mechanisms." *Italian Geotechnical Journal*, 4, 11–31.

Cascini, L., Guida, D., Nocera, N., Romanzi, G., and Sorbino, G. (2000). "A preliminary model for the landslides of May 1998 in Campania Region." *Proc., 2nd Int. Symp. on Geotechnics of Hard Soil-Soft Rock*, Vol. 3, Balkema, Naples, Italy, 1623–1649.

Cascini, L., and Sorbino, G. (2002). "Soil suction measurement over large areas: a case study." *Proc., 3rd International Conference on Unsaturated Soils*, Vol. 2, Recife, Brazil, 829–834.

Cascini, L., Sorbino, G., and Cuomo, S. (2003). "Modelling of flowslides triggering in pyroclastic soils." *Proc., Int. Conf. on "Fast Slope Movements—Prediction and Prevention for Risk Mitigation"*, L. Picarelli, ed., Vol. 1, Patron, Bologna, 93–100.

Chu, J., Leroueil, S., and Leong, W. K. (2003). "Unstable behaviour of sand and its implications for slope instability." *Can. Geotech. J.*, 40, 873–885.

Crosta, G. B., and Dal Negro, P. (2003). "Observations and modelling of soil slip-debris flow initiation processes in pyroclastic deposits: the Sarno 1998 event." *Nat. Hazards Earth Syst. Sci.*, 3, 53–69.

Cruden, D. M., and Varnes, D. J. (1996). "Landslide types and processes." *Transportation Research Board Special Rep. No. 247*, A. K. Turner and R. L. Schster, eds., Landslides Investigation and Mitigation, National Research Council, National Academy Press, Washington D.C., 36–75.

Cuomo, S. (2006). "Geomechanical modelling of triggering mechanisms for flow-like mass movements in pyroclastic soils." Ph.D. dissertation, Univ. of Salerno, Italy, 274.

Dai, F., Lee, C. F., Wang, S., and Feng, Y. (1999). "Stress-strain behaviour of a loosely compacted volcanic-derived soil and its significance to rainfall-induced fill slope failures." *Eng. Geol. (Amsterdam)*, 53, 359–370.

Darve, F., and Laouafa, F. (2000). "Instabilities in granular materials and application to landslides." *Mech. Cohesive-Frict. Mater.*, 5(8), 627–652.

De Vita, P., Celico, P., Siniscalchi, M., and Panza, R. (2006). "Distribution, hydrogeological features and landslide hazard of pyroclastic soils on carbonate slopes in the area surrounding Mount Somma-Vesuvius (Italy)." *Italian Journal of Engineering Geology and Environment*, 1, 75–98.

De Vita, P., and Reichenbach, P. (1998). "Rainfall-triggered landslides: A reference list." *Environ. Geol.*, 35(2–3), 219–233.

Dietrich, W. E., Reneau, S. L., and Wilson, C. J. (1986). "Hollows, colluvium and landslides in soil-mantled landscapes." *Hillslope processes*, A. D. Abrahamas, ed., Allen and Unwin, Boston, 361–388.

Duncan, J. M. (1996). "State of the art: Limit equilibrium and finite element analysis of slopes." *J. Geotech. Engrg.*, 122(7), 577–596.

Eckersley, D. (1990). "Instrumented laboratory flowslides." *Geotechnique*, 40, 489–502.

Ekanayake, J. C., and Philipps, C. J. (2002). "Slope stability thresholds for vegetated hillslopes: a composite model." *Can. Geotech. J.*, 39, 849–862.

Fell, R., Hungr, O., Leroueil, S., and Riemer, W. (2000). "Keynote lecture—Geotechnical engineering of the stability of natural slopes, and cuts and fills in soil." *GeoEng 2000*, Vol.1, Technomic, Lancaster, Penn., 21–120.

Fernandez Merodo, J. A., Pastor, M., Mira, P., Tonni, L., Herreros, M. I., Gonzalez, E., and Tamagnini, R. (2004). "Modelling of diffuse failure mechanisms of catastrophic landslides." *Comput. Methods Appl. Mech. Eng.*, 193, 2911–2939.

Fiorillo, F., and Wilson, R. C. (2004). "Rainfall induced debris flows in pyroclastic deposits, Campania (Southern Italy)." *Eng. Geol. (Amster-*

*dam)*, 75, 263–289.
Fredlund, D. G., Morgenstern, N. R., and Widger, R. A. (1978). "The shear strength of unsaturated soils." *Can. Geotech. J.*, 15, 313–321.
Fuchu, D., Lee, C. F., and Sijing, W. (1999). "Analysis of rainstorm-induced slide-debris flows on natural terrain of Lantau Island, Hong Kong." *Eng. Geol. (Amsterdam)*, 51, 279–290.
Futai, M. M., Lacerda, W. A., and Almeida, M. S. S. (2004). "Evolution of gully processes in unsaturated soils." *Landslides: Evaluation and Stabilization*, Vol. 2, W. A. Lacerda, M. Ehrlich, S. A. B. Fontoura, and A. S. F. J. Sayao, eds., Taylor and Francis, London, 1019–1025.
Geoslope. (2005). "User's guide." *GeoStudio 2004, version 6.13*, Geo-Slope Int. Ltd., Calgary, Canada.
Guida, D. (2003). "The role of the zero-order basin in flowslide-debris flow occurrence and recurrence in Campania (Italy)." *Proc., Int. Conf. on Fast Slope Movements—Prediction and Prevention for Risk Mitigation*, Vol. 1, L. Picarelli, ed., Patron, Bologna, Italy, 93–100.
Hungr, O. (2004). "Flow slides and flows in granular soils." *Proc., Int. Workshop "Flows 2003—Occurrence and Mechanisms of Flows in Natural Slopes and Earthfill"*, L. Picarelli, ed., Patron, Bologna.
Hungr, O., Evans, S. G., Bovis, M. J., and Hutchinson, J. N. (2001). "A review of the classification of landslides of the flow type." *Environ. Eng. Geosci.*, VII(3), 221–238.
Hutchinson, J. N. (1988). "Morphological and Geotechnical parameters of Landslides in relation to Geology and Hydrogeology. State of the art report." *Proc., V Int. Symp. on Landslides*, Vol. 1, Lausanne, Switzerland, 3–35.
Iverson, R. M. (2000). "Landslide triggering by rain infiltration." *Water Resour. Res.*, 36(7), 1897–1910.
Iverson, R. M., Reid, M. E., and LaHusen, R. G. (1997). "Debris flow mobilization from landslides." *Annu. Rev. Earth Planet. Sci.*, 25, 85–138.
Janbu, N. (1954). "Application of composite slip surface for stability analysis." *Proc., European Conference on Stability of Earth Slopes*, Stockholm, Sweden, 3, 43–49.
Johnson, K. A., and Sitar, N. (1990). "Hydrologic conditions leading to debris-flow initiation." *Can. Geotech. J.*, 27, 789–801.
Lacerda, W. A. (2004). "The behaviour of colluvial slopes in a tropical environment." *Landslides: Evaluation and Stabilization*, W. A. Lacerda, M. Ehrlich, S. A. B. Fontoura, and A. S. F. J. Sayao, eds., Vol. 2, Taylor and Francis, London, 1315–1342.
Lade, P. V. (1992). "Static instability and liquefaction of loose fine sandy slopes." *J. Geotech. Engrg.*, 118(1), 51–71.
Laouafa, F., and Darve, F. (2002). "Modelling of slope failure by a material instability mechanism." *Comput. Geotech.*, 29, 301–325.
Leroueil, S. (2001). "Natural slopes and cuts: movement and failure mechanisms." *Geotechnique*, 51(3), 197–243.
Leroueil, S. (2004). "Geotechnics of slopes before failure." *Landslides: Evaluation and Stabilization*, W. A. Lacerda, M. Ehrlich, S. A. B. Fontoura, and A. S. F. J. Sayao, eds., Vol. 1, Taylor and Francis, London, 863–884.
Lourenco, S., Sassa, K., and Fukuoka, H. (2006). "Failure process and hydrologic response of a two layer physical model: Implications for rainfall-induced landslides." *Geomorphology*, 73(1–2), 115–130.
Malkawi, A. I. H., Hassan, W. F., and Sarma, S. K. (2001). "Global search method for locating general slip surface using Monte Carlo technique." *J. Geotech. Geoenviron. Eng.*, 127(8), 688–698.
Matsushi, Y., Hattanji, T., and Matsukura, Y. (2006). "Mechanisms of shallow landslides on soil-mantled hillslopes with permeable and impermeable bedrocks in the Boso Peninsula, Japan." *Geomorphology*, 76, 92–108.
Mira McWilliams, P. (2002). "Análisis por Elementos Finitos de Problemas de Rotura en Geomateriales." Ph.D. thesis, Escuela Técnica Superior de Ingenieros de Caminos, Canales y Puertos, Universidad Politécnica de Madrid.
Montgomery, D. R., Dietrich, W. E., Torres, R., Anderson, S. P., Heffner, J. T. and Loague, K. (1997). "Piezometric response of a steep unchanneled valley to natural and applied rainfall." *Water Resour. Res.*, 33, 91–109.
Morgenstern, N. R., and Price, V. E. (1965). "The analysis of the stability of general slip surfaces." *Geotechnique*, 15(1), 79–93.
Ng, C. W. W. (2008). "Deformation and failure mechanisms of loose and dense fill slopes with and without soil nails." *Landslides and engineered slopes*, Z. Chen, J.-M. Zhang, K. Ho, F.-Q. Wu, and Z.-K. Li, eds., Taylor and Francis, London, 159–177.
Ng, C. W. W., and Shi, Q. (1998). "Influence of rainfall intensity and duration on slope stability in unsaturated soils." *Quarterly Journal of Engineering Geology and Hydrogeology*, 31(2), 105–113.
Olivares, L., and Damiano, E. (2007). "Postfailure mechanics of landslides: Laboratory investigation of flowslides in pyroclastic soils." *J. Geotech. Geoenviron. Eng.*, 133(1), 51–62.
Olivares, L., and Picarelli, L. (2003). "Shallow flowslides triggered by intense rainfalls on natural slopes covered by loose unsaturated pyroclastic soils." *Geotechnique*, 53(2), 283–287.
Onda, Y., Tsujimura, M., and Tabuchi, H. (2004). "The role of subsurface water flow paths on hillslope hydrological processes, landslides and landform development in steep mountains of Japan." *Hydrol. Process.*, 18, 637–650.
Pastor, M., Fernandez-Merodo, J. A., Gonzalez, E., Mira, P., Li, T., and Liu, X. (2004). "Modelling of landslides: (I). Failure mechanisms." *Degradations and instabilities in geomaterials, CISM course and lectures No. 461*, F. Darve and I. Vardoulakis, eds., Springer, New York, 287–317.
Pastor, M., Haddad, B., Sorbino, G., Cuomo, S., and Drempetic, V. (2008). "A depth-integrated, coupled SPH model for flow-like landslides and related phenomena." *Int. J. Numer. Analyt. Meth. Geomech.*, 33(2), 143–172.
Pastor, M., Quecedo, M., Fernandez-Merodo, J. A., Herreros, M. I., Gonzalez, E., and Mira, P. (2002). "Modelling tailing dams and mine waste dumps failures." *Geotechnique*, 52(8), 579–591.
Picarelli, L. et al. (2004). "A research on rainfall-induced flowslides in unsaturated soils of pyroclastic origin." *Landslides: Evaluation and stabilization*, Taylor and Francis, London, 1, 1497–1506.
Reid, M. E. (1997). "Slope instability caused by small variations in hydraulic conductivity." *J. Geotech. Geoenviron. Eng.*, 123, 717–725.
Revellino, P., Hungr, O., Guadagno, F. M., and Evans, S. G. (2004). "Velocity and runout prediction of destructive debris flows and debris avalanches in pyroclastic deposits, Campania region, Italy." *Environ. Geol.*, 45, 295–311.
Richards, L. A. (1931). "Capillary conductions of liquids through porous mediums." *J. Appl. Phys.*, 1, 318–333.
Schuster, R. L., and Highland, L. M. (2007). "The Third Hans Cloos Lecture. Urban landslides: socioeconomic impacts and overview of mitigative strategies." *Bull. Eng. Geol. Environ.*, 66, 1–27.
Sladen, J. A., D'Hollander, R. D., and Krahn, J. (1985). "The liquefaction of sands, a collapse surface approach." *Can. Geotech. J.*, 22, 564–578.
Sorbino, G. (2005). "Numerical modelling of soil suction measurements in pyroclastic soils." *Int. Symp. Advanced Experimental Unsaturated Soil and Mechanics*, Taylor and Francis, London, 541–547.
Sorbino, G., and Foresta, V. (2002). "Unsaturated hydraulic characteristics of pyroclastic soils." *Proc., 3rd Int. Conf. on Unsaturated Soils*, Vol. 1, Swets and Zeitlinger, Lisse, 405–410.
Take, W. A., Bolton, M. D., Wong, P. C. P., and Yeung, F. J. (2004). "Evaluation of landslide triggering mechanisms in model fill slopes." *Landslides*, 1, 173–184.
Tsaparas, I., Rahardjo, H., Toll, D. G., and Leong, E. C. (2002). "Controlling parameters for rainfall-induced landslides." *Comput. Geotech.*, 29, 1–27.
Van Asch, Th. W. J., Malet, J. P., and van Beek, L. P. H. (2006). "Influence of landslide geometry and kinematic deformation to describe the liquefaction of landslides: Some theoretical considerations." *Eng. Geol. (Amsterdam)*, 88, 59–69.
Wang, F. W., Sassa, K., and Wang, G. (2002). "Mechanism of a long-runout landslide triggered by the August 1998 heavy rainfall in Fukushima Prefecture, Japan." *Eng. Geol. (Amsterdam)*, 63, 169–185.
Wang, G., and Sassa, K. (2001). "Factors affecting rainfall induced land-

slides in laboratory flume tests." *Geotechnique*, 51, 587–600.

Wang, G., and Sassa, K. (2003). "Pore-pressure generation and movement of rainfall-induced landslides: effects of grain size and fine-particle content." *Eng. Geol. (Amsterdam)*, 69, 109–125.

Yamamuro, J. A., and Lade, P. J. (1998). "Steady-state concepts and static liquefaction of silty sands." *J. Geotech. Geoenviron. Eng.*, 124(9), 868–878.

Yasufuku, N., Ochiai, H. and Hormdee, D. (2005). "An empirical relationship for evaluating collapsible settlements of volcanic ash sandy soil." *Advanced experimental unsaturated soil mechanics*, A. Tarantino, E. Romero, and Y. J. Cui, eds., Taylor and Francis, London, 265–272.

Zhang, J., Jiao, J. J., and Yang, J. (2000). "In situ rainfall infiltration studies at a hillside in Hubei Province, China." *Eng. Geol. (Amsterdam)*, 57, 31–38.

Zienkiewicz, O. C., Chan, A. H. C., Pastor, M., Shrefler, B. A., and Shiomi, T. (1999). *Computational geomechanics*, Wiley, New York.

Zienkiewicz, O. C., Chang, C. T., and Bettess, P. (1980). "Drained, undrained, consolidating dynamic behaviour assumptions in soils." *Geotechnique*, 30, 385–395.